International Biodeterioration & Biodegradation 160 (2021) 105210

Contents lists available at ScienceDirect

International Biodeterioration & Biodegradation

journal homepage: www.elsevier.com/locate/ibiod

Heterotrophic nitrification-aerobic denitrification performance in a granular sequencing batch reactor supported by next generation sequencing

Paula Bucci [a], Bibiana Coppotelli [b], Irma Morelli [b,c], Noemí Zaritzky [a,d], Alejandro Caravelli [a,*]

[a] Centro de Investigación y Desarrollo en Criotecnología de Alimentos, CIDCA, (CCT – La Plata – CONICET, Facultad de Ciencias Exactas, UNLP, CIC), 47 y 116, B1900AJJ, La Plata, Argentina
[b] Centro de Investigación y Desarrollo en Fermentaciones Industriales, CINDEFI, (UNLP, CCT-La Plata, CONICET), Buenos Aires, Argentina
[c] CIC-PBA, La Plata, Argentina
[d] Facultad de Ingeniería, Universidad Nacional de la Plata, Argentina

ARTICLE INFO

Keywords:
Heterotrophic nitrification
Aerobic denitrification
Online monitoring
Bacterial Composition
PYCRUSt
Next generation sequencing

ABSTRACT

Several nitrogen transformation processes occur in wastewater treatment; among them, heterotrophic nitrification-aerobic denitrification (HNAD) has not been adequately quantified. In the present study, a comprehensive analysis of the simultaneous ammonia and organic carbon removal was carried out in an aerobic granular sequencing batch reactor (SBR) operated under feast/famine regime. For this, biological processes, microbial community composition and metabolic pathways were evaluated. Mass balances allowed estimating the ammonia assimilation and simultaneous nitrification and denitrification (SND). Better SND process (55%) was achieved in starvation period involving that denitrification driven by intracellular carbon reserves is more efficiently coupled to the ammonia oxidation with regard to external carbon-driven denitrification. Proton balances and titration monitored the organic carbon and nitrogen removal. High abundance of HNAD bacteria, *Diaphorobacter* sp. and *Flavobacterium* sp., and *Zoogloea* sp. aerobic denitrifier was detected by next generation sequencing (NGS) technology. Bioinformatics analysis predicted enzymes involved in nitrogen transformation pathways present in Phylogenetic investigation PYCRUSt database. Heterotrophic nitrification took place involving detoxification against ammonia. Non-limiting nitrate and high oxygen concentrations were favorable for aerobic denitrifiers. HNAD was the main process responsible for the biological nitrogen removal according to NGS and operational conditions given by high dissolved oxygen and low COD:NO_3^--N ratio.

1. Introduction

Simultaneous nitrification and denitrification (SND) has been proposed about two decades ago for wastewaters treatment; SND takes place in one reactor reducing costs (Chai et al., 2019). This process requires the coexistence of autotrophic nitrifying and denitrifying bacteria. Nitrification occurs at the surface of microbial flocs or granules and denitrification occurs in the anoxic center. However, the nitrogen removal efficiency of the SND process strongly depends on the oxygen concentration (Third et al., 2003a). Newly, heterotrophic nitrification and aerobic denitrification (HNAD) has been proposed as an interesting alternative for nitrogen removal since nitrification and denitrification occurs simultaneously under aerobic conditions (Khanichaidecha et al., 2019). Novel strains of heterotrophic ammonia oxidizing bacteria (AOB) with ability of ammonia oxidation coupled to aerobic denitrification capabilities has been detected (Padhi et al., 2017). Heterotrophic nitrifying bacteria show higher growth rates and nitrogen removal efficiency than autotrophs (Jin et al., 2019; Khanichaidecha et al., 2019).

The effects of different physicochemical factors on the HNAD process has been mainly evaluated for microbial isolates obtained from environmental samples and wastewater treatment systems. Optimal conditions for ammonia removal and growth are different for each HNAD bacterium; however, higher growth and ammonia removal are commonly reported at: pH = 6.0–9.0, carbon/nitrogen ratio = 7.5–12, temperature = 20–30 °C, and simple carbon source such as sodium pyruvate, sucrose, sodium acetate, sodium citrate, sodium succinate and glucose (Lei et., 2016; Wang et al., 2017; Li et al., 2019a; Silva et al., 2019). In wastewater treatment systems, growth of heterotrophic nitrifiers is favored at high organic carbon and nitrogen loads (Zhao et al., 2013); however, these bacteria can also grow at low COD and low COD:

* Corresponding author.
E-mail address: alejandrocaravelli@hotmail.com (A. Caravelli).

https://doi.org/10.1016/j.ibiod.2021.105210
Received 5 May 2020; Received in revised form 15 March 2021; Accepted 16 March 2021
Available online 5 April 2021

N ratio (Chai et al., 2019). In many systems, reactors are operated with alternating phases of organic carbon availability and starvation, known as feast/famine regime, which can affect the composition of the microbial community. It has been reported that the decrease of the feast/famine ratio favors the enrichment of heterotrophic nitrifiers, while autotrophs are reduced (Li et al., 2019b). In natural environments and engineered systems, several groups of microorganisms can contribute to the nitrogen removal process. In an anthropogenically-impacted environment (oil sands pit lake) nitrification was performed by autotrophic AOBs and heterotrophic AOBs (Mori et al., 2019). In effluent treatment plants, several microbial groups related to the nitrogen metabolism are found, such as autotrophic nitrifiers, anaerobic denitrifiers, anaerobic ammonium oxidation (ANNAMOX) bacteria and HNAD bacteria (Silva et al., 2019). In biofilm SBR, nitrogen removal by conventional autotrophic nitrifiers and denitrifiers, aerobic denitrifiers and HNAD bacteria has been reported (Chai et al., 2019). In these complex communities the contribution of each microbial group to the global process of nitrogen removal should be analyzed.

In order to carry out SND, an organism must possess key genes for nitrification and denitrification (Pal et al., 2015). Two possible metabolic pathways have been proposed to explain the HNAD process. One involves oxidation of ammonia to hydroxylamine, followed by oxidation to nitrite (nitrate), which is reduced progressively to nitric oxide, nitrous oxide and molecular nitrogen. The other pathway involves the conversion of ammonia to nitrogenous gas via intermediate hydroxylamine i.e. oxidation of ammonia to hydroxylamine is followed by conversion to nitrous oxide and finally molecular nitrogen (Zhao et al., 2012; Huang et al., 2013; Lei y col., 2016). These probable metabolic pathways have been deduced mainly from enzyme assays with cell-free extracts of bacterial isolates. In few studies, some key genes involved in conventional nitrification and denitrification processes have been identified in HNAD using polymerase chain reaction (PCR) amplification (Barman et al., 2017; Wang et al., 2017; Lang et al., 2019). However, in most HNAD bacteria the absence of some key genes or the participation of other genes could not be demonstrated (Jin et al., 2019). For mixed communities, potential metabolic pathways have been also proposed. Conversion of ammonia to molecular nitrogenous via hydroxylamine has been suggested for heterotrophic nitrifiers in aerobic granular sludge (Li et al., 2019b). Functional genes for nitrification and denitrification have been detected for an unclassified gammaproteobacterial group (Mori et al., 2019). However, metabolic pathways and mechanisms of SND must be clarified (Jin et al., 2019).

Molecular biological techniques allow evaluating the dominant members of the microbial communities. The advent of the new generation of mass sequencing technologies, NGS (next generation sequencing), allows to analyze the differences in each system with respect to the microbial composition. NGS are very strong technologies that not only shed light on the composition of the community but also on the functional characteristics and the relationship between the microbial community and environmental factors (Langenheder et al., 2010).

Biological systems enriched in heterotrophic nitrifiers could offer many advantages such as an excellent nitrification and SND capacity. However, the stability of these systems can be altered by deficiencies in the aeration, pH changes, and toxic entry, which could cause an irreversible effect. Early detection of failures is particularly important for those most susceptible biological processes such as nitrification. The application of control strategies for key biological processes would allow the optimal operation of the reactor. Titration is a simple and economical method that has been proposed for the monitoring of biological processes (Guisasola et al., 2007). This method consists in the indirect measurement of the rate of consumption or production of protons through the quantification of the volumes of acid or base respectively, which are dosed to the reactor to maintain a constant pH. This is possible since biological processes strongly influence the pH of the environment.

The objectives of the present work are: a) To propose a simple method, based on proton balances and titration, for monitoring removal of organic carbon and nitrogen in an aerobic granular sequencing batch reactor (SBR) with heterotrophic nitrification-denitrification, b) To evaluate the composition of the complex bacterial community in the SBR by applying next generation sequencing technology (NGS) and predict microbial functions, c) To determine the possible metabolic pathways of nitrogen removal in the granular system.

2. Materials and methods

2.1. Reactor and synthetic effluent

A SBR with a height of 100 cm and an internal diameter of 10.86 cm was used with a work volume of 4.6 L. The air was supplied by aerators and distributed through diffusers located at the reactor bottom. A synthetic influent containing ($g.L^{-1}$): ammonium sulfate (0.564–0.815), monobasic potassium phosphate (0.065), dibasic potassium phosphate (0.051) and sodium acetate (1.566) was used. Synthetic wastewater was supplemented with two trace element solutions, which were described by Bucci et al. (2020). A 1 mL volume of each trace element solution was added to 1 L of synthetic wastewater.

The SBR was operated with consecutive cycles involving the following phases: feeding (1 min), reaction (1432 min), sedimentation (5 min), draining (1 min) and idle (1 min). Cycle time was 24 h. The inoculum corresponded to activated sludge from a laboratory-scale SBR fed with the described wastewater. Synthetic wastewater (2.3 L) was fed to the reactor at the start of each operational cycle. Mixed liquor was withdrawn at the end of the aerobic phase resulting a cellular retention time (CRT) of 20 days. After the settling period, treated wastewater was removed from the SBR. The hydraulic retention time (HRT) was 2 days and the volumetric exchange ratio was 50%.

The SBR was operated under conditions that favor granulation: superficial upflow air velocity of 2.3 cm s^{-1} and sludge settling time of 5 min pH was automatically controlled (7.5 ± 0.1) using acid (H_2SO_4, 0.91 M) and basic (NaOH, 0.5 M) solutions. The dissolved oxygen concentration was about 7.5 mg $O_2.L^{-1}$.

Two experimental conditions were set: Condition 1 presented a volumetric nitrogen loading rate of 60 mg NH_3-N.$(L.day)^{-1}$, volumetric organic loading rate of 600 mg COD.$(L.day)^{-1}$, volumetric inorganic phosphorous loading rate of 12 mg PO_4^--P.$(L.day)^{-1}$ resulting in a COD: N:P ratio of 100:10:2. Condition 2 had the following volumetric loading rates: of 90 mg NH_3-N.$(L.day)^{-1}$, 600 mg COD.$(L.day)^{-1}$ and 12 mg PO_4^--P.$(L.day)^{-1}$ equivalent to COD:N:P ratio of 100:15:2.

2.2. Analytical methods

2.2.1. Determination of organic substrate and biomass

The chemical oxygen demand (COD) of the mixed liquor (CODt, total COD) and filtered samples (<0.45 μm) of the reactor (CODs, soluble COD) was determined. Soluble COD was used as a measure of the concentration of acetate. The biomass concentration expressed as COD (CODb, biomass COD) was obtained from the difference between CODt and CODs. COD determinations were carried out using a commercial kit (HACH, method 8000). The biomass concentration was also determined as total solids (TS). In this method, samples were taken from the mixed liquor of the reactor, which were centrifuged and resuspended in distilled water. This washing process was performed twice. The samples were placed in an oven (105 °C) for 24 h. The biomass concentration (X_T) was expressed as g $TS.L^{-1}$. The values obtained were correlated with the CODb measurements. COD is a rapid method of biomass measurement in comparison with the TS methodology. However, in order to perform the SVI test and to determine specific rates of different chemical parameter it is necessary to know the value of TS. For this reason, the correlation between these two methods allows to have quickly TS values at different stages of the study.

2.2.2. Sludge volume index (SVI) and granule size

The biomass settling properties were evaluated by the sludge volume index (SVI_{30}, mL.g TS^{-1}). The particle size distribution of the biomass was determined using Mastersizer 2000E (Malvern Instruments Worcestershire, UK).

2.2.3. Determination of ammonia (NH_3-N), nitrate (NO_3^--N) and nitrite (NO_2^--N)

Concentrations of ammonia, nitrate and nitrite of the reactor were determined using filtered samples of the mixture liquor (<0.45 μm). NH_3-N, NO_3^--N and NO_2^--N were determined by HACH methods. Inorganic nitrogen (Ni) corresponds to the sum of the concentrations of NH_3-N, NO_3^--N and NO_2^--N.

2.2.4. Determination of kinetic parameters and removal efficiency of ammonia nitrogen and inorganic nitrogen

The volumetric uptake rates of NH_3-N ($r_{NH3\text{-}N}$, mg NH_3-N.$(L.h)^{-1}$) and COD uptake (CODs, mg CODs.$(L.h)^{-1}$) were determined from the slope of the decay curves of NH_3-N and CODs vs. time. The specific rates of NH_3-N uptake ($q_{NH3\text{-}N}$, mg NH_3-N.$(g\ TS.h)^{-1}$) and COD uptake (qCODs, mg COD.$(g\ TS.h)^{-1}$) were also determined. The volumetric production rates of nitrite ($r_{NO2\text{-}N}$, mg NO_2^--N.$(L.h)^{-1}$) and nitrate ($r_{NO3\text{-}N}$, mg NO_3^--N.$(L.h)^{-1}$) were obtained from the slope of the NO_2^--N and NO_3^--N curves respectively. Specific production rates of nitrite ($q_{NO2\text{-}N}$, mg NO_2^--N.$(g\ TS.h)^{-1}$) and nitrate ($q_{NO3\text{-}N}$, mg NO_3^--N. $(g\ TS.h)^{-1}$) were also calculated. All kinetic parameters were determined at the initial stage of the feast and starvation periods, at different CRT.

The ammonia N removal (NH_3-N_R) was determined by the following expression:

$$\%NH_3 - N_R = \left(\frac{(NH_3 - N)_O - (NH_3 - N)_F}{(NH_3 - N)_O}\right)100 \quad (1)$$

where $(NH_3\text{-}N)_O$ and $(NH_3\text{-}N)_F$ correspond to the concentrations of ammonia nitrogen (mg NH_3-N.L^{-1}) at the beginning and the end of the operating cycle respectively.

The inorganic N removal (Ni_R) was determined as follows:

$$\%Ni_R = \left(\frac{Ni_O - Ni_F}{Ni_O}\right)100 \quad (2)$$

where Ni_O is the concentration of inorganic nitrogen of the reactor at the start of the operating cycle (mg.L^{-1}) and Ni_F is the Ni concentration (mg.L^{-1}) at the end of cycle (effluent from SBR). Ni_F is the sum of NH_3-N, NO_2^--N, and NO_3^--N. The nitrate and nitrite concentrations at the beginning of the cycle (from the remaining supernatant of the preceding cycle) were not considered in the determination of the Ni_O concentration.

2.2.5. Consumption and production of protons (H^+)

pH value of the reactor was monitored. For maintaining a constant pH value of 7.5, acid (H_2SO_4, 0.91 M) or base (NaOH, 0.5 M) solutions were added to the reactor using peristaltic pumps that were automatically controlled by a pH control system. A titration technique based on the consumption and production of protons (H+) was implemented to evaluate the process of ammonia removal by nitrifying activity. For this, the doses of the acid and base solutions, necessary to maintain the constant pH in the reactor, were measured.

Proton production/consumption (HP, mmol H^+), for a given period, was calculated using the following expression (Guisasola et al., 2007).

$$HP = V_{base}\ C_{base} - V_{acid}\ C_{acid} \quad (3)$$

where V_{base} and V_{acid} represent the consumed volumes of base and acid solutions (mL) and C_{base} and C_{acid} represent their concentrations respectively (M).

HP was determined every 15 min throughout each operational cycle. Proton production/consumption rates (rHP, mmol H^+.$(L.h^{-1})$) were determined from the slope of the HP curves as a function of time.

2.2.6. Respirometry

Oxygen uptake rate (OUR) was determined by closed respirometry. Assays were carried out at 20 °C following a modification of the ISO 8192 method. The respirometer consisted of a sealed flask with an oxygen electrode (YSI Model 58), magnetic stirring and an aerator. Data from the oxygen electrode were recorded every 20 s during about 5 min. Samples from the SBR (20 mL) were placed in the respirometer and aerated for about 2 min. Then, the aeration was stopped and the decrease in the dissolved oxygen concentration was recorded as a function of time. The slope of the straight line corresponds to the total OUR (rO_{2T}, mg O_2.$(L.h)^{-1}$).

2.2.7. Determination of total carbohydrates (TC) and polyhydroxyalkanoates (PHAs)

The total carbohydrates (TC) concentration of the biomass was determined by the Anthrone method. In biological processes with feast/famine regime, glycogen is commonly cycled and it is assumed that changes in the concentration of TC occur on the glycogen component (Zheng et al., 2009). Extraction and quantification of PHA from biomass were performed following the method proposed by Venkateswar Reddy et al. (2012).

2.3. Carbon and nitrogen balance of the SBR process

Nitrogen can be oxidized by nitrifying activity or used for heterotrophic growth. Identification of each process is very difficult by two reasons: a) active biomass increases slightly during the feast period of each operating cycle, and cannot be satisfactorily detected by gravimetry, b) nitrite and/or nitrate generated by nitrifying activity can be simultaneously denitrified, and consequently, the nitrification process could be underestimated.

A mass balance of the organic substrate and different forms of inorganic nitrogen was proposed in order to quantify the contribution of each biological process to the global nitrogen removal. In addition, the mass balance would allow estimating both the denitrifying activity and the SND process.

2.3.1. Feast phase: mass balances for acetate, nitrogen and oxygen

Third et al. (2003b), working with an aerobic/anoxic SBR, have proposed that acetate consumed by the bacteria is used for oxidation, PHB production and assimilation into biomass during aerobic phase. In the present study, it was proposed that acetate can be used by the heterotrophic bacteria for glycogen and PHA production, oxidative phosphorylation (ATP generation), assimilation into biomass and denitrification. For simplification, complete denitrification i.e. reduction of nitrate to nitrogen gas was assumed to occur. For the feast phase, a modification of the electron balance proposed by Third et al. (2003b) was used, including glycogen production and denitrification. The balance was expressed in COD units as follows:

$$rCOD_S = rGly_F + 1.125\ rPHA_F + rO_{2H} + 1.05\ rX + 1.25\ r(NO_3^- - N)_D \quad (4)$$

where $rCOD_S$ is the organic substrate uptake rate (mmol O_2.$(L.h)^{-1}$), $rGly_F$ is the glycogen production rate from acetate (mmol Gly.$(L.h)^{-1}$), $rPHA_F$ is the PHA production rate from acetate (mmol PHA.$(L.h)^{-1}$), rO_{2H} is the oxygen uptake rate corresponding to the heterotrophic metabolism (mmol O_2.$(L.h)^{-1}$), rX corresponds to the heterotrophic growth rate from acetate (mmol X.$(L.h)^{-1}$), and $r(NO_3^-\text{-}N)_D$ is the denitrification rate (mmol NO_3^--N.$(L.h)^{-1}$). All the parameters were expressed in COD units (mmol O_2.$(L.h)^{-1}$) using the following conversion factors: 1 mol O_2.C-mol Gly^{-1}, 1.125 mol O_2.C-mol PHB^{-1}, 1.05 mol O_2.C-mol X^{-1}, 1.25 mmol O_2.mmol NO_3^--N^{-1} (For details see

Supplementary data).

Oxygen uptake rate involved two processes, nitrification (rO_{2N}) and acetate oxidation by heterotrophs (rO_{2H}). For simplification, the following assumptions were made: full nitrification from ammonia to nitrate (without denitrification via nitrite), and complete denitrification from nitrate to N_2 (For details see Supplementary data). It should be noted that even though full nitrification was assumed to occur, the nitrite oxidation rate may be lower than the ammonia oxidation rate causing nitrite accumulation. Therefore, the mass balance involved both steps of the nitrification process then nitritation and nitratation rates were estimated separately.

According to these assumptions, the following expressions were proposed:

$$rO_{2N} = y_{O/N1} r(NH_3 - N)_{Ox} + y_{O/N2} r(NO_2^- - N)_{Ox} \quad (5)$$

$$rO_{2H} = rO_{2T} - y_{O/N1} r(NH_3 - N)_{Ox} - y_{O/N2} r(NO_2^- - N)_{Ox} \quad (6)$$

$$r(NO_2^- - N)_{Ox} = r(NH_3 - N)_{OX} - r(NO_2^- - N)_{AC} \quad (7)$$

$$r(NO_3^- - N)_D = r(NO_2^- - N)_{Ox} - r(NO_3^- - N)_{AC} \quad (8)$$

where $y_{O/N1}$ is the stoichiometric coefficient for the ammonia oxidation (1.5 mol O_2.mol NH_3-N^{-1}), $r(NH_3\text{-}N)_{ox}$ is the ammonia oxidation rate (mol NH_3-N.$(L.h)^{-1}$), $y_{O/N2}$ is the stoichiometric coefficient for the nitrite oxidation (0.5 mol O_2.mol NO_2^--N^{-1}), $r(NO_2^-\text{-}N)_{ox}$ is the nitrite oxidation rate (mol NO_2^--N.$(L.h)^{-1}$), rO_{2T} is total rO_2 determined by closed respirometry, $r(NO_2^-\text{-}N)_{AC}$ corresponds to the nitrite accumulation rate (mol NO_2^--N.$(L.h)^{-1}$), $r(NO_3^-\text{-}N)_D$ is the denitrification rate (mol NO_3^--N.$(L.h)^{-1}$) and $r(NO_3^-\text{-}N)_{AC}$ corresponds to the nitrate accumulation rate (mol NO_3^--N.$(L.h)^{-1}$).

Combining Equations (7) and (8) the following equation was obtained:

$$r(NO_3^- - N)_D = r(NH_3 - N)_{OX} - r(NO_2^- - N)_{AC} - r(NO_3^- - N)_{AC} \quad (9)$$

For ammonia, the following balance was proposed:

$$r(NH_3 - N)_T = r(NH_3 - N)_X + r(NH_3 - N)_{OX} \quad (10)$$

where $r(NH_3\text{-}N)_T$ is the total ammonia uptake rate (mol NH_3-N.$(L.h)^{-1}$)), $r(NH_3\text{-}N)_X$ corresponds to the ammonia uptake rate for heterotrophic growth (mol NH_3-N.$(L.h)^{-1}$), being $r(NH_3\text{-}N)_X = rX.y_{N/X}$; $y_{N/X}$ corresponds to the stoichiometric coefficient that relates the nitrogen and carbon contents of the biomass (0.2 mol N.C-mol X^{-1}, for $CH_{1.8}O_{0.5}N_{0.2}$).

The heterotrophic growth rate rX was estimated from Eq. (4). Combining Equations (4), (6), (7), (9) and (10), replacing $r(NH_3\text{-}N)_X$ by $rX.y_{N/X}$, and rearranging equations, heterotrophic growth rate from acetate and ammonia could be estimated for the feast phase by means of the following expression:

$$rX = \frac{rCOD_S + r(NH_3 - N)_T\left(y_{O/N1} + y_{O/N2} - 1.25\right) + 1.25\, r(NO_3^- - N)_{AC} + r(NO_2^- - N)_{AC}\left(1.25 - y_{O/N2}\right) - (rO_{2T} + rGly_F + 1.125\, rPHA_F)}{y_{N/X}\left(y_{O/N1} + y_{O/N2}\right) + \left(1.05 - 1.25\, y_{N/X}\right)} \quad (11)$$

2.3.2. Famine phase: mass balances for endogenous organic carbon, nitrogen and oxygen

Intracellular carbon reserves (glycogen and PHA), from feast phase, were used as carbon and energy sources for microbial growth, ATP generation by oxidation, and denitrification during the starvation period. The following balance (COD units) was proposed:

$$rGly_D + 1.125\ rPHA_D = 1.05\ rX + rO_{2H} + 1.25\ r(NO_3^- - N)_D \quad (12)$$

where $rGly_D$ is the glycogen degradation rate (mmol Gly.$(L.h)^{-1}$), and $rPHA_D$ is the PHA degradation rate (mmol PHA.$(L.h)^{-1}$).

For the mass balances of ammonia and oxygen, Equations (5)–(10) are valid. Combining Equations (6), (7), (9), (10) and (12) and rearranging equations heterotrophic growth rate from intracellular carbon reserves could be estimated by means of the following expression:

$$rX = \frac{rGly_D + 1.125\, rPHA_D + r(NH_3 - N)_T\left(y_{O/N1} + y_{O/N2} - 1.25\right) - r\,O_{2T} + 1.25\, r(NO_3^- - N)_{AC} + r(NO_2^- - N)_{AC}\left(1.25 - y_{O/N2}\right)}{y_{N/X}\left(y_{O/N1} + y_{O/N2} - 1.25\right) + 1.05} \quad (13)$$

For both periods feast and starvation, once rX has been estimated, the ammonia uptake rate for heterotrophic growth $r(NH_3\text{-}N)_X$ was calculated as $rX.y_{N/X}$. Finally, the ammonia oxidation rate $r(NH_3\text{-}N)_{ox}$ was estimated by using Eq. (10).

All kinetic parameters were determined for the initial phase of each period, feast and starvation, and all operating cycles for conditions 1 and 2 were analyzed.

For all assays, ammonia removal by SND was estimated as follows:

$$\%SND = \left(\frac{r(NH_3 - N)_{OX} - r(NO_X - N)}{r(NH_3 - N)_{OX}}\right) 100 \quad (14)$$

where $r(NO_X\text{-}N)$ corresponds to the sum of $r(NO_2^-\text{-}N)_{AC}$ and $r(NO_3^-\text{-}N)_{AC}$.

2.4. Proton production/consumption rates (rHP)

In aerobic activated sludge systems, the main processes that influence pH are the following: nitrification, carbon source uptake, CO_2 generation from respiration, ammonia uptake and CO_2 stripping by aeration (Gernaey et al., 2002). The production or consumption of protons (H^+) associated with the uptake of acetate and ammonia depends on the equilibrium reactions of each chemical species (Guisasola et al., 2007).

Acetic acid (HAC) in solution is partially dissociated according to the following reaction:

$$HAC \rightleftarrows AC^- + H^+ \quad (15)$$

HAC and AC^- are the undissociated and dissociated forms respectively. The acetate uptake by heterotrophic bacteria leads to the H^+ consumption (basification of the system). This is due to the fact that the microorganisms consume the undissociated form of the acid, and H^+ is consumed by the backward reaction (Pratt et al., 2004). This proton consumption would imply pH increase if this parameter was not automatically controlled in the reactor. Protons can be measured by means of

the acid addition when the titrimetric technique is applied (Gernaey et al., 2002). The rate of H^+ consumption associated with the HAC uptake (rHP_{HAC}, mmol H^+.$(L.h)^{-1}$) depends on its pK_{AC} (4.8) and the pH of the system (7.5) according to the following expression (modified from Guisasola et al., 2007):

$$rHP_{HAC} = -\left(\frac{rHAC}{1 + 10^{(pKAC-pH)}}\right) \quad (16)$$

where rHAC corresponds to the acetate uptake rate expressed as mmol HAC.$(L.h)^{-1}$ (H^+ consumption associated with the acetate uptake). For this, $rCOD_S$ (mmol O_2.$(L.h)^{-1}$) was converted to mmol HAC units using the conversion factor 0.5 mmol HAC.mmol O_2^{-1}.

The undissociated acetic acid fraction decreases as the pH increases. Acetic acid is mostly in the dissociated form at pH close to neutrality (Guisasola et al., 2007). Therefore, at pH 7.5 a high H^+ consumption rate caused by the acetate uptake is expected in the present study. Ammonia consumption also took place in the SBR. Ammonia is a weak base (pK_{NH3} = 9.25), which is mostly in protonated form (NH_4^+) in the pH range close to neutrality. Microbial consumption of ammonia generates acidification. The H^+ production rate of this process (rHP_{NH3}, mmol H^+.$(L.h)^{-1}$) was estimated as follows (modified from Guisasola et al., 2007):

$$rHP_{NH_3} = \left(\frac{r(NH_3 - N)_T}{1 + 10^{(pKNH_3-pH)}}\right) \quad (17)$$

where $r(NH_3\text{-}N)_T$ is the total ammonia uptake rate (mmol N.$(L.h)^{-1}$).

Nitritation, the first stage of the nitrification process, also contributes to the acidification of the system according to the following expression:

$$2\ NH_4^+ + 3\ O_2 \rightarrow 2NO_2^- + 2H_2O + 4H^+ \quad (18)$$

According to this reaction, rHP corresponding to the nitrification process (rHP_N, mmol H^+.$(L.h)^{-1}$) can be calculated as follows: $2{\cdot}r(NH_3\text{-}N)_{OX}$. For this, $r(NH_3\text{-}N)_{OX}$ must be estimated from the difference between $r(NH_3\text{-}N)_T$ (mmol N.$(L.h)^{-1}$) and $r(NH_3\text{-}N)_X$ (mmol N.$(L.h)^{-1}$) (Eq. (10)). The NH_4^+:H^+ ratio proposed in Eq. (18) has been successfully used to measure nitrification rates in systems operated with nitrogen control by pH sensors (Massone et al., 1998).

Denitrification contributes to the basification of the system; this process neutralizes approximately half of the acidity generated by nitrification. In the denitrification process with NO_3^--N as electron acceptor, it has been previously assumed that one H^+ is taken up per NO_3^- ion that pass the cell wall as HNO_3 is a strong acid (Petersen et al., 2002). According to these authors, in our study rHP of denitrification (rHP_D, mmol H^+.$(L.h)^{-1}$) was estimated as: $-1{\cdot}r(NO_3^-\text{-}N)_D$ (mmol N.$(L.h)^{-1}$).

The production and stripping of CO_2 contribute to the generation and loss of H^+ respectively according to the equilibrium reaction of carbonic acid (Guisasola et al., 2007). CO_2 is produced from the oxidation of acetate, glycogen and PHA; the aeration generates continuous stripping of CO_2. rHP associated with the net production of CO_2 (rHP_{CO2}, mmol H^+.$(L.h)^{-1}$) corresponds to the difference between the production processes and CO_2 stripping.

Finally, the rHP resulting from the combination of the processes of nitrification and denitrification corresponded to $rHP_{N+D} = rHP_N + rHP_D$ (mmol H^+.$(L.h)^{-1}$); rHP_{HAC} and rHP_D present negative values implying consumption of H^+ (basification); rHP_{NH3} and rHP_N have positive values (acidification). rHP_{CO2} can present positive or negative values depending on the prevalent phenomenon, production or stripping of CO_2. rHP_{CO2} (mmol H^+.$(L.h)^{-1}$) can be estimated from the rHP balance, based on the contribution of all the biological and physical-chemical processes involved, according to the following expression:

$$rHP_{Total} = rHP_{HAC} + rHP_{NH_3} + rHP_{N+D} + rHP_{CO_2} \quad (19)$$

where rHPtotal (mmol H^+.$(L.h)^{-1}$) is the rHP value determined by titration.

2.5. DNA extraction and SEQUENCing

The microbial genomic DNA from the bioreactor was extracted in duplicate utilizing an E.Z.N.A DNA kit (OMEGA, USA) following the manufacturer's protocol and stored at −80 °C until analysis. The V3 hypervariable region of the 16S rRNA gene was amplified using 341F/518R primer combination 5′CCTACGGGAGGCAGCAG3' and 5′ATTACCGCGGCTGCTGG 3′ (Li et al., 2009). The amplification was performed following the protocol described by Kim et al. (2017). The Microbiome Helper workflow was used to estimate the bacterial taxonomic abundance in the 16S rRNA datasets of microbial DNA of the SBR and functional roles in terms of KOs (Kegg orthology) (Comeau et al., 2017): this includes the use of QIIME (Caporaso et al., 2010), FastQC (v0.11.5) (http://www.bioinformatics.babraham.ac.uk/projects/fastqc/), and PEAR (v0.9.10) (Zhang et al., 2014) in the first steps in order to evaluate raw reads, identify ambiguous reads, and stitch them together. After chimeric screening and removal using VSEARCH (v1.11.1) (Rognes et al., 2016) and UCHIME algorithm (Edgar et al., 2011) respectively, open-reference OTU picking (OTU, operational taxonomic units), was performed at 97% identity using SortMeRNA (Kopylova et al., 2012) and SUMACLUST (Mercier et al., 2013) and reads were clustered against the Greengenes database. Prior to the normalization of the final OTU table, low confidence OTUs were removed. Finally, the diversity of the consortium in the SBR was assessed.

16S rRNA gene sequences of the microbial community have been deposited in GenBank with accession numbers: PRJNA532854.

2.6. PYCRUSt functional prediction

PYCRUSt (Phylogenetic Investigation of Communities by Reconstruction of Unobserved States) is a bioinformatics software package designed to predict metagenome functional content from marker gene (e.g., 16S rRNA) surveys and full genomes (Langille et al., 2013). During Qiime workflow a BIOM file was formated to be used as an input for PYCRUSt (Langille et al., 2013). PYCRUSt (v1.1.0) was used to infer the functional potential of prokaryotic communities in terms of KEGG orthology and pathways, and to associate taxonomic changes with functional differences (Langille et al., 2013). The OTU table was used as the input file for the metagenome prediction. Major steps for the bioinformatics protocol include: a) Reducing the OTU table to just the reference OTUs, b) Normalizing the OTU table by predicted 16S copy numbers, c) Predicting abundances of KEGG orthology (KOs) in each sample, d) Collapsing KOs into KEGG Pathways defined at level 1, level 2 and level 3 (Kyoto Encyclopedia of Genes and Genomes, http://www.genome.jp/kegg/). (Kanehisa et al., 2012) Orthology (KO), e) Connecting the OTUs that are contributing to each KO of interest. STAMP (v2.1.3) was used for data visualization and statistical analyses (Parks et al., 2014). The Nearest Sequenced Taxon Index (NSTI) score, which is the sum of phylogenetic distances for each OTU between its nearest relative with a sequenced reference genome, measured in terms of substitutions per site in the 16S rRNA gene and weighted according to the frequency of that OTU, was used as an indicator for the accuracy of PYCRUSt.

3. Results

3.1. Stability of the systems: granules size and SVI

The reactor was initially operated with a volumetric nitrogen load of 60 mg NH_3-N.$(L.day)^{-1}$ (condition 1). System stability in terms of granule size and settling properties was achieved after about 80 days of operation (4 CRT). At steady-state, average granule size was 0.4 mm; SVI = 20 mL g TS^{-1} and biomass concentration was 1.9 g $TS.L^{-1}$. Similarly, at condition 2 (nitrogen load = 90 mg NH_3-N.$(L.day)^{-1}$), granular stability was reached after about 80 days of operation. At steady-state, average granule size was 1.2 mm, SVI = 5 mL g TS^{-1} and

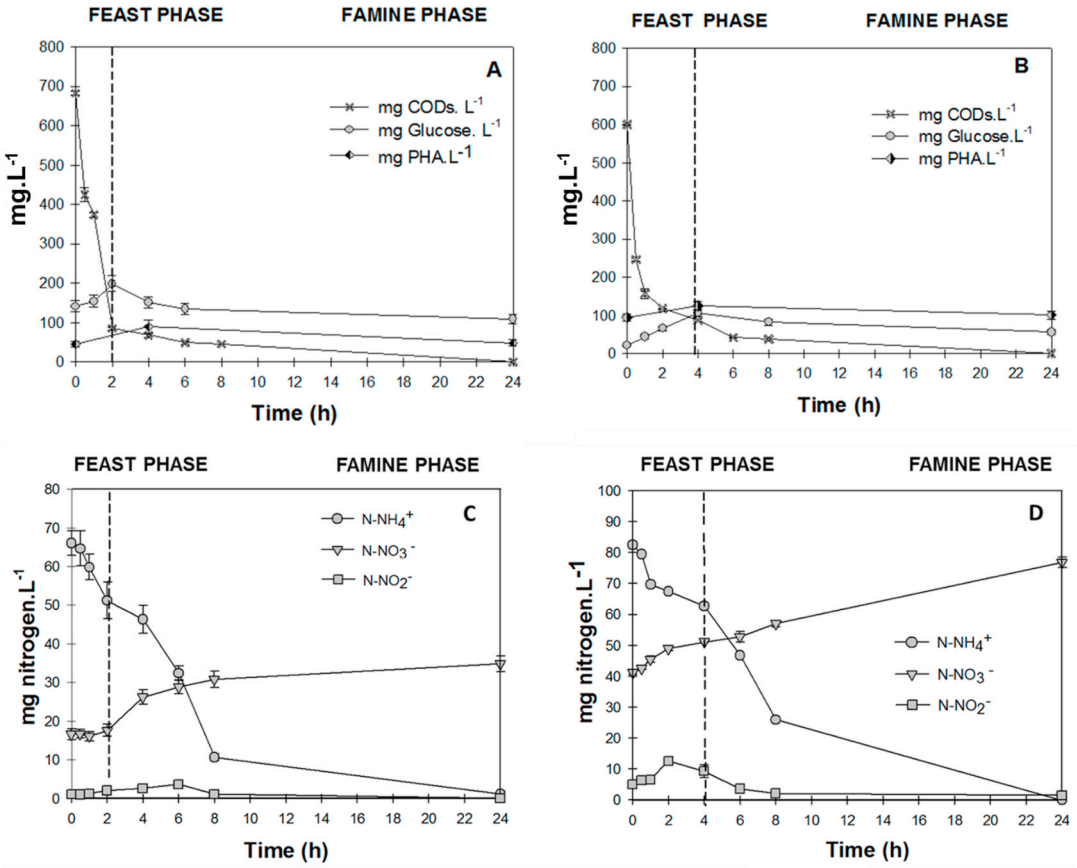

Fig. 1. Changes in the concentrations of soluble COD, glycogen, PHA and different forms of inorganic nitrogen throughout an operating cycle of the steady-state SBR. Condition 1 (A and C) and Condition 2 (B and D). CODs (x), glucose (●), PHA (◆), NH_3-N (●), NO_3^--N (▼), NO_2^--N (■).

biomass concentration reached 2.3 g $TS.L^{-1}$.

3.2. Organic carbon uptake and nitrification of the systems

SBR was operated under two COD/N ratios (condition 1: COD:N:P ratio of 100:10:2 and condition 2: 100:15:2). The organic substrate (soluble COD) and ammonia were completely removed under both conditions (Fig. 1A–D). In the first hours of the operating cycles, about 90% of the organic substrate was removed. This period of external carbon availability corresponded to the feast period (Fig. 1A and B). Under both operating conditions, accumulation of glycogen and PHA, as intracellular carbon reserves, took place from acetate during the feast period. After the external carbon source was almost exhausted, glycogen and PHA were degraded throughout the starvation period (Fig. 1A and B). Thus, starvation period corresponded to the phase without external organic carbon, in which intracellular carbon reserves are used for all metabolic processes related to cellular maintenance and growth.

In condition 1, oxidized forms of N (nitrite and nitrate) did not increase significantly during the feast period. A priori it could be assumed that there was no nitrifying activity in that period. Nitrification was evident in the starvation period, in which progressive increase of the NO_3^- concentration took place until the end of the operating cycle; NO_2^- was slightly generated (Fig. 1C). In condition 2, the nitrifying activity took place during the entire operating cycle. Nitrite accumulation was observed between 0 and 2 h of the cycle, then nitrite concentration decreased to very low levels which cannot be detected by the spectrophotometric method used. Nitrate increased progressively throughout the entire operating cycle (Fig. 1D). It should be taken into account that in both conditions 1 and 2, the initial nitrite and nitrate concentrations (i.e. at 0 h of the operational cycle) corresponded to about half of the concentrations at the end of the cycle (24 h), this is because the volumetric exchange ratio in the reactor was 50%.

In both conditions, complete NH_3-N removal was achieved; inorganic N removal was about 50% in both cases (Table 1). Contributions of each process, nitrification and assimilation, to the total ammonia removal were quantified from mass balances (See Section 3.3).

The specific rate of soluble COD uptake was similar for both conditions. In the starvation period, the initial uptake rate of NH_4^+-N for condition 2 was about 2 times higher than that obtained in condition 1 (Table 1). In condition 2, a higher concentration of initial NH_3-N probably favored nitrifying activity, without affecting the soluble COD heterotrophic uptake. Free ammonia (FA, NH_3) reached peak concentrations of 1.23 mg/L (SD = 0.15) and 1.85 mg/L (SD = 0.12) for conditions 1 and 2 respectively. Low values of free nitrous acid (FNA, HNO_2) were estimated in both conditions (<0.004 mg/L).

Table 1
Efficiency of N removal and kinetic parameters.

Operating cycle	Parameters	Condition 1 (100:10:2)	Condition 2 (100:15:2)
Total Cycle	% Removal of NH_4^+-N	100	100
	% Removal of inorganic N	51.61 (4.84)	48.50 (0.88)
Feast Phase	rCODs (mg COD_S. $(L.h)^{-1}$)	352.15 (21.43)	422.33 (24.09)
	qCODs (mg COD_S. $(g\ TS.h)^{-1}$)	184.00 (17.50)	183.62 (14.1)
Starvation Phase	$r(NH_3\text{-}N)_T$ (mg NH_3-N. $(L.h)^{-1}$)	4.10 (0.57)	9.00 (0.98)
	$q(NH_3\text{-}N)_T$ (mg NH_3-N. $(g\ TS.h)^{-1}$)	2.15 (0.35)	3.90 (0.42)

3.3. Nitrogen assimilation, nitrification and SND

In the present study, acetate was used for oxidation, PHB production and assimilation into biomass during the feast phase, as proposed by Third et al. (2003b). In addition, acetate was also used for glycogen production and denitrification. Glycogen production during the feast phase was demonstrated in Section 3.2 for both conditions 1 and 2. Nitrate reduction was observed in some operational cycles at the start of feast phase (data not shown). Thus, mass balance proposed (Eq. (4)) was applied.

From estimations of $r(NH_3\text{-}N)_X$ and $r(NH_3\text{-}N)_{OX}$, by means of Equations (10), (11) and (13), the contribution of nitrification and assimilation processes to the total nitrogen removal was determined. For this, firstly the total ammonia uptake rate ($r(NH_3\text{-}N)_T$) was determined experimentally for feast and starvation periods. Then, the ammonia uptake rate for heterotrophic growth ($r(NH_3\text{-}N)_X$) was calculated as rX. $y_{N/X}$, being rX previously estimated by Equations (11) and (13) for feast and starvation periods respectively. Finally, $r(NH_3\text{-}N)_{OX}$ was estimated from the difference between $r(NH_3\text{-}N)_T$ and $r(NH_3\text{-}N)_X$ using Equation (10). $r(NH_3\text{-}N)_{OX}$ is the ammonia oxidation rate attributed to nitrifiers. Ammonia removed by nitrification corresponded to 0.0 ± 0.0% and 70.0 ± 7.5% of the removed ammonia for feast and starvation periods respectively (condition 1). In condition 2, nitrification represented 30.0 ± 3.7% and 76.2 ± 11.9% of the total ammonia removal process for feast and starvation periods respectively. In both conditions, the rest of ammonia was removed by assimilation. The %SND obtained for condition 1 was 0.0 ± 0.0% and 54.0 ± 4.8% for feast and starvation periods respectively. In condition 2, %SND was 23.0 ± 2.7% and 55.0 ± 5.6% for each period respectively.

3.4. Proton production/consumption rates (rHP) for the SBR monitoring

For both conditions 1 and 2, the different kinetic parameters (rHP) were calculated considering the initial (linear) part of the feast and starvation periods for all the operating cycles. Total rHP of the SBR was determined by titration throughout each operating cycle. For both conditions, during the first hours, a linear decrease in HP (consumption of H^+) took place, due to the acetate uptake by the heterotrophic bacteria (Feast period). In the starvation period, continuous production of H^+ (linear increase) took place for both conditions, which was mainly associated with the nitrification. A linear correlation between rHP_{Total} and rHP_{HAC} was found, which includes the values corresponding to the feast period of all operating cycles for both conditions ($rHP_{HAC} = 0.722.rHP_{Total} + 0.161$, $R^2 = 0.936$). For the starvation period, a linear correlation was found between the values obtained of rHP_{TOTAL} and rHP_{N+D} for all operating cycles of both conditions ($rHP_{N+D} = 0.795.rHP_{TOTAL} - 0.038$, $R^2 = 0.937$). Table 2 shows the mean rHP values of all biological and physicochemical parameters estimated for steady-state operating cycles of conditions 1 and 2. It can be seen that the proton consumption caused by the CODs uptake is the process that most strongly influences on the pH change (feast period). The mean rHP_{HAC} value for condition 1 does not differ significantly from that corresponding to condition 2. According to this result, it was previously shown that the CODs uptake rates r_{CODs} were similar for both conditions (Table 1).

Regarding to rHP_N and rHP_{N+D} values, in the case of the condition 1, the nitrification and denitrification processes became relevant once almost all the acetate was consumed (starvation period). In the condition 2, nitrification, although it was not the main process, began in the feast period, leading to the nitrate production (Fig. 1D). Relevant rHP_N and rHP_{N+D} values were estimated for the feast period of condition 2 (Table 2). The production of H^+ associated with the consumption of NH_3 was insignificant. In the feast period, of both conditions, a net loss of CO_2 took place leading to a consumption of H^+ (negative rHP_{CO2}, Table 2). Stripping prevails over the processes of CO_2 metabolic production, causing loss of the buffer capacity of the system by continuous removal of the bicarbonate from the wastewater.

Table 2
Mean rHP values corresponding to all the biological and physicochemical parameters estimated for steady-state operating cycles of conditions 1 and 2.

$mmol\ H^+.(L.h)^{-1}$	CONDITION 1		CONDITION 2	
	FEAST	FAMINE	FEAST	FAMINE
rHP_{TOTAL}	−3.78 (0.5)	0.73 (0.07)	−4.08 (0.54)	0.86 (0.09)
rHP_{NH3}	$0.06E^{-1}$ ($0.80E^{-2}$)	$0.04E^{-1}$ ($0.80E^{-2}$)	$0.05E^{-1}$ ($0.10E^{-1}$)	$0.09E^{-1}$ ($0.70E^{-2}$)
rHP_N	0.00 (0.00)	0.44 (0.04)	0.70 (0.02)	0.89 (0.09)
rHP_D	0.00 (0.00)	−0.12 (0.01)	−0.20 (0.02)	−0.25 (0.03)
rHP_{N+D}	0.00 (0.00)	0.32 (0.05)	0.5 (0.01)	0.64 (0.06)
rHP_{HAC}	−2.81 (0.44)	−0.08 (0.07)	−3.10 (0.23)	−0.20 (0.10)
rHP_{CO2}	−1.03 (0.24)	0.49 (0.05)	−1.53 (0.60)	0.40 (0.32)

3.5. Analysis of bacterial composition of the granules

A metabarcoding analysis (Mercier et al., 2013) was carried out to determine the composition and relative abundances of bacterial populations present in the bioreactor. Considering that both assayed conditions of the SBR led to similar performances regarding inorganic nitrogen and ammonia removal for total cycle and %SND for starvation period, the analysis was carried out in the reactor operating under condition 1 (COD:N:P ratio = 100:10:2). This study allowed us to propose a potential relationship between the processes of simultaneous nitrogen and carbon removal and the microorganisms likely involved in those biological processes.

High performance sequencing of the 16S rRNA gene PCR fragments was performed from the total DNA extracted from the granular biomass present in the SBR. The extraction allowed to evaluate 59250 sequences grouped in 813 OTU. All representative sequences of each OTU were classified within the Bacteria domain. The relative frequency revealed the presence of 6 main bacterial orders (Fig. 2 A), among which 15 main genera prevailed (Fig. 2 B). The most abundant phyla found in the SBR were Proteobacteria representing 72% and Bacteroidetes 25%. In a lower proportion, we found, Verrucomicrobia (2%), Plantinomycetes and Actinobacteria (representing less than 1%).

Within the phylum Proteobacteria, the most abundant orders found were: Rhodocyclales, Burkholderiales, Sphingomonadales and Xanthomonadales (Fig. 2B).

In relation to the processes that are occurring in the bioreactor, a potential correlation with the function of the microorganisms found in the DNA analysis can be predicted. Regarding the process of inorganic nitrogen removal, many bacteria belonging to the phylum proteobacteria have a metabolism able of degrading inorganic nitrogen and accumulating and degrading reserve substances. The order Rhodocyclales has an important influence in nitrate reduction (Pacheco-Sánchez et al., 2019). The Rhodocyclales order showed several genera in high abundance, being *Dechloromonas* (8.1%) and *Zoogloea* (43.2%) the most representative. The genus *Dechloromonas* is characterized by being a dominant denitrifying (Han et al., 2019) with excellent ability to remove different species of inorganic nitrogen. *Zoogloea* exhibits periplasmic nitrate reductase genes (Huang et al., 2015) that have an extremely high metabolic rate of ammonia removal compared to other nitrifying genera. It is known, that denitrifying activity of *Zoogloea* is stimulated by high availability of ammonia. Zhang et al. (2017) showed that the Burkholderiales order (specifically the genus *Diaphorobacter*) has the enzymes necessary to carry out both heterotrophic nitrification and aerobic denitrification. *Diaphorobacter* showed high abundance in the present study (4.2%). Xanthomonadales (genus *Lysobacter*) represents the last relevant order of phylum proteobacteria in the present study. It has already been described by Saijai et al. (2016) the relevance of this order on the nitrification process. Many members of the Rhodocyclales order could contribute to the nitrogen removal process of the present study; however, the degree of participation of each genus could not be determined by means of the genomic analysis carried out.

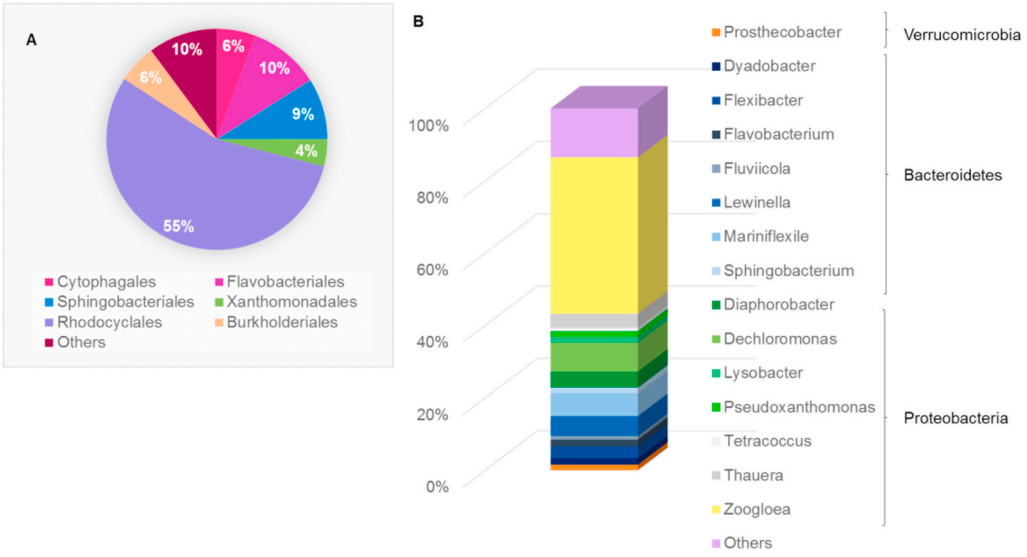

Fig. 2. Differences in relative abundance at the order level in the SBR (A). Only reads that represented more than 2% are shown. Relative phylotype frequency at the genus level as revealed by Illumina sequencing in the SBR. Genera with <1% reads belonging to each phylum were grouped in "Others" (B).

Within phylum Bacteroidetes, the most relevant orders found in the present study were: Sphingobacteriales and Flavobacteriales. Sphingobacteriales is known by the ability to fix CO_2 and degrade organic matter. Yang et al. (2019) from the study of the UJ101 strain of Flavobacteriales, demonstrated that this order is able to reduce nitrate and participate in denitrification processes. The relevant genera within this phylum were *Flavobacterium* (1.9%) and *Dyadobacter* (1.78%). *Flavobacterium* shows aerobic denitrifying ability (Pishgar et al., 2019; Deng et al., 2020). This genus is able to oxidize hydroxylamine; therefore it has been also identified as HNAD bacteria (Castignetti and Hollocher, 1984). Baskaran et al. (2020) reported that *Flavobacterium* sp. has been found in NOB enrichment from sediments of aquaculture pond. *Dyadobacter* can oxidize ammonia to nitrite (Harun et al., 2020). *Dyadobacter* sp. showed high ammonia removal capacity in pure culture and mixed culture in the aquaculture wastewater treatment (Neissi et al., 2020). These authors suggested that the ammonia removal would involve its conversion to nitrite by this bacterial genus.

Conventional autotrophic nitrification by AOBs like *Nitrosomonas* and *Nitrobacter* was detected in very small percentages. AOBs showed a relative abundance of about 0.61% and NOBs represented 0.16% (Table S4 in supplementary data).

3.5.1. *Assessing contribution of SBR bacterial populations to main biological processes*

The prediction obtained by PYCRUSt, using the Greengenes database, revealed 35 KEGG Orthologs (KO). These KOs belong to functional genes of the bacterial OTUs, corresponding to the most relevant genera found in the SBR, involved in the metabolic pathways of inorganic nitrogen degradation and carbon fixation (Fig. S2, supplementary data). However, we have found other KOs, with relevant functions in the nitrogen cycle, in less abundant genera of the system. All information that contributes to demonstrate the functions of each of the enzymes represented in terms of KO is available as supplementary data (Table S5). For a proper interpretation, the KO analysis has been made at the order level as presented below. Visualization of the KO distribution between orders is shown in Fig. S2.

According to the prediction of PYCRUSt and analyzing the most abundant genera in the system, Rhodocyclales was considered the main functional bacterial group able to perform the nitrogen fixation, mediated by key reactions catalyzed by nitrogenase enzymes (K02586, K02588 and K02591) (Figs. S2–A and Table S5). A minor contribution for K02591 by Sphingomonadales and Burkholderiales was observed. Rhodocyclales was probably the main contributor of enzymes involved in the reduction of dissimilatory nitrate and in the denitrification process. This is mainly observed by the presence of the nitrite reductase enzyme represented by the following KO: K00368 and K00363, and nitrate reductase enzyme represented by K00370, K00371, K00374, K02567 and K02568.

Denitrification was also represented by the enzyme periplasmic nitrate reductase NapA (K02567), nitric oxide reductase, cytochrome c-containing subunit II (K02305) and nitric oxid subunit B (K04561) which were found in the order Rhodocyclales. The recently mentioned KOs were also significantly found in the order Xantomonadales, mainly K04561 and K00363, which are involved in the denitrification and dissimilatory nitrate reduction respectively (Figs. S2–A and Table S5). The enzyme K00376, which plays a role in the denitrification process, has been found in various orders Rhodocyclales, Cytophagales, Burkholderiales, Rhizobiales, and Flavobacteriales (Fig. S2).

Ammonia monooxygenases (AMO) enzymes catalyze oxidation of ammonia to hydroxylamine (K10944, K10945, K10946). These enzymes are also involved in the following cycles: methane metabolism, nitrogen metabolism and carbon metabolism. Enzymes responsible of the hydroxylamine oxidation to nitrite and finally nitrate were also detected in orders with low proportion. K10535 (hydroxylamine dehydrogenase) for example was detected in Nitrospirales and Nitrosomonadales order. This enzyme, responsible of the hydroxylamine oxidation to nitrite, has been found in Nitrospirales among others orders (De Voogd et al., 2015).

It should be noted that PYCRUSt allows predicting the potential abundance of each enzyme, represented in terms of KO, related to the biological processes of interest as well as the possible microbial groups that can provide such enzymes. However, neither the active participation of detected bacterial genera nor the synthesis of predicted enzymes in the studied system can be actually determined.

In relation to carbon fixation related enzymes, adenylylsulfate kinase (K00720) was contributed only by Xantomonadales order (Figs. S2–B and Table S5). In relation to carbon flux: glycolysis/gluconeogenesis enzymes like myo-inositol 2-dehydrogenase (K00010) were predicted only for Cytophagales order. Enzymes related to hydroxypropionate-hydroxybutylate cycle and dicarboxylate-hydroxybutyrate cycle (K00626) were predicted in the six bacterial phylotypes present in the SRB. Enzymes associated to dicarboxylate-hydroxybutyrate cycle were contributed mainly by Rhodocyclales, followed by Flavobacteriales and Xantomonadales. They are succinyl-CoA synthetase alpha and beta subunit (K01902, K01903), succinate dehydrogenase (K00239, K00240

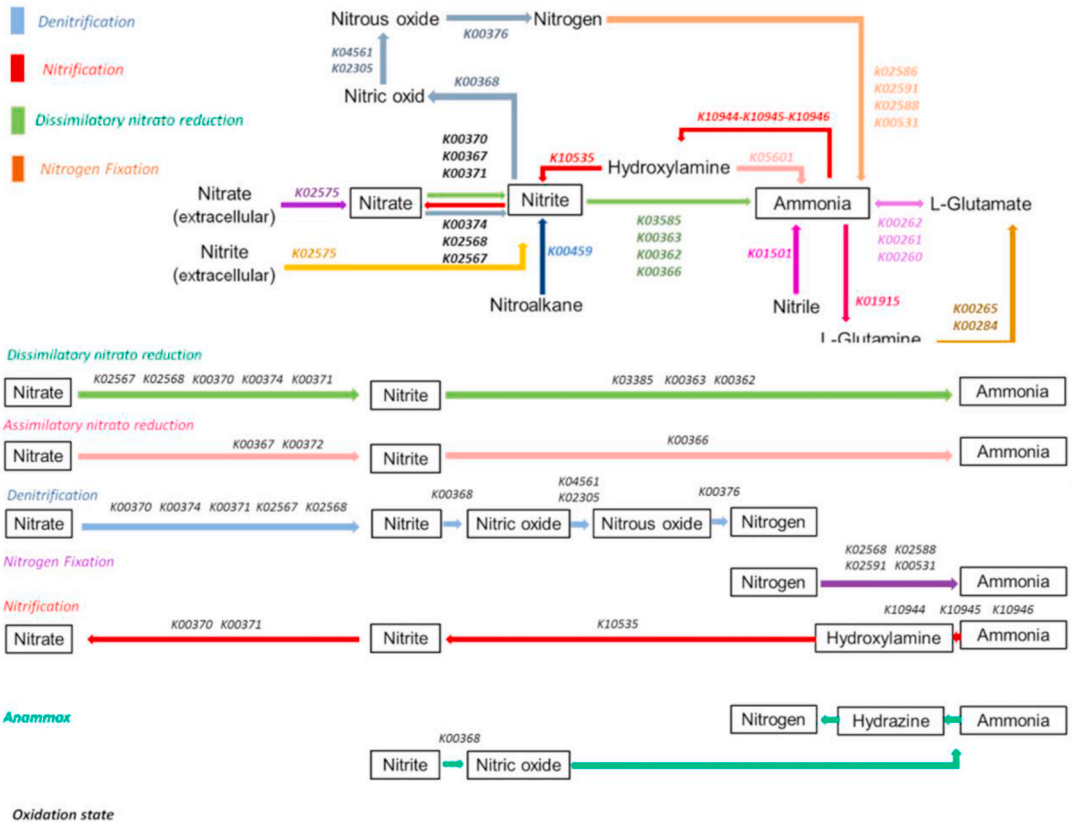

Fig. 3. Schematic model of functional genes involved in nitrogen metabolism encoded in the genome of the microorganisms.

and K00241), malate dehydrogenase (K00024), fumarate hydratase (K01595, K01676) and phosphoenolpyruvate carboxylase (K01007) (Figs. S2–B and Table S5). It must be considered that the hydroxypropionate–hydroxybutyrate and dicarboxylate–hydroxybutyrate cycles occur in anaerobic and aerobic Crenarchaeota; however, these autotrophic microorganisms were not found in the present study. Most enzymes related to the dicarboxylate-hydroxybutyrate cycle are also found in the Krebs cycle of bacteria, therefore the enzymes mentioned above would be related to the aerobic metabolism of bacteria.

A schematic model of functional genes involved in nitrogen metabolism predicted by PYCRUSt to be encoded in the genome of the microorganisms is shown in Fig. 3. Different processes linked to nitrogen metabolism could take place: nitrification, nitrogen fixation, dissimilatory nitrate reduction and denitrification.

4. Discussion

A higher volumetric nitrogen load (90 mg NH_3-N.(L.day)$^{-1}$), equivalent to COD:N:P ratio of 100:15:2 (condition 2), led to an ammonia removal rate about twice the corresponding to condition 1 (60 mg NH_3-N.(L.day)$^{-1}$), COD:N:P ratio = 100:10:2). A mass balance allowed determining the importance of the heterotrophic nitrification and SND processes. In condition 1, during the feast phase, there was no nitrifying activity. Nitrification and SND processes were relevant in starvation period. In condition 2, at the highest nitrogen load, nitrification and SND processes took place from the beginning of the operating cycle. In addition higher levels of ammonia were not toxic to nitrifiers, but rather favored the nitrifying activity. It is widely accepted that autotrophic bacteria are more sensitive to toxic agents than heterotrophs. In addition, within the autotrophs, nitrite oxidizing bacteria (NOB) are more sensitive to free ammonia (FA) and free nitrous acid (FNA) than ammonia oxidizing bacteria (AOB). A comparative analysis of literature values for FA inhibition of NOB showed that threshold concentrations for the inhibition ranged between 0.02 and 0.5 mg NH_3-N.L^{-1}, with 50–100% inhibition for concentrations between 1 and 24 mg NH_3-N.L^{-1} (Philips et al., 2002). *Nitrosomonas*, a typical AOB, was not inhibited by 16 mg NH_3-N.L^{-1} (Vadivelu et al., 2007). For FNA, *Nitrobacter*, a typical NOB, begins to be inhibited at 0.01 mg HNO_2-N.L^{-1}; inhibition of *Nitrosomonas* starts at 0.08–0.10 mg HNO_2-N.L^{-1} (Vadivelu et al., 2007). Few studies have evaluated the effect of FA and FNA on heterotrophic nitrifiers. Ammonia oxidation by heterotrophic AOB (*Paracoccus* sp.) was negatively affected to concentrations higher than 120 mg NH_3-N.L^{-1}; FA levels 1.5–5.5 mg NH_3-N.L^{-1} inhibited NOBs (Liu et al., 2018). In the present study, the FNA levels were lower than the inhibition threshold reported in literature for both autotrophic AOBs and NOBs; however, FA levels are within the range of inhibition of autotrophic NOBs. In condition 2, the highest initial FA levels could negatively affect the NOBs, which could explain the nitrite accumulation at the beginning of the cycle (Fig. 1D). FA concentrations were below the typical levels of AOB inhibition.

Mass balances allowed determining that the nitrification and SND rates are significantly favored at higher nitrogen load (COD:N = 100:15, condition 2). In this condition, low %SND was estimated for the feast period, being the denitrification process driven by acetate. Acetate in feast period was mainly used for microbial growth and glycogen and PHA storage and to a lesser extent for denitrification. In starvation period, a high fraction of the nitrate generated was simultaneously denitrified, using intracellular reserves as carbon source. This led to a % SND of about 55%, which was similar to that corresponding to the condition 1. In the starvation period, degradation of intracellular reserves could be coupled to the ammonia oxidation leading to a more efficient SND process than that corresponding to the feast period.

In feast period, a linear correlation between rHP_{Total} and rHP_{HAC} values with slope close to 1 was found for both conditions. This correlation allows inferring that acetate uptake strongly influences the pH change, which agrees with results reported by Gernaey et al. (2002) who

found a linear relationship between the added acetate and the amount of H^+ consumed in batch aerobic degradation tests. According to the results of the present study, in the feast period, HAC uptake could be quickly monitored by determining the H^+ consumption rate. Similarly, for the starvation period, a linear correlation with slope close to 1 was found between the values obtained of rHP_{TOTAL} and rHP_{N+D} for both conditions. This strong correlation allows verifying that the nitrification-denitrification processes are the most relevant in the studied systems. In the starvation period, the H^+ production rate associated with the nitrification process (rHP_N) in condition 2, was about twice the corresponding to condition 1. rHP_D for condition 2 was also twice that of condition 1, indicating that the denitrifying activity was also favored at a higher nitrogen load. The rHP_{N+D} values were also highest in condition 2 (Table 2). The higher nitrogen load favored the SND rate, but did not imply an increase in the percentage removal of N (Table 1). This result may be due to the fact that the volumetric load applied in condition 2 was 50% greater than that corresponding to condition 1.

Through the PYCRUSt analysis, it was also possible to corroborate the potential existence of enzymes responsible of the nitrate formation in the SBR (Fig. 3). Key enzymes involved in the nitrification process were also predicted. It is possible that in addition to the KOs related to the nitrification process like K10944, K10945 and K10946, there are other KOs species involved in HNAD that could not be detected in the system because PYCRUSt is an interactive Python Shell that presents a specific database by default.

Only a limited number of functional genes can be predicted, since when the 16S rRNA sequence is not present in databases, the bioinformatics programs used do not provide information on the physiological capabilities of the unknown organism. Ammonia monooxygenases (AMO) enzyme corresponded probably to autotrophic AOB; however, AMO could also be contributed by heterotrophic nitrifiers provided that these enzymes are also included in the PYCRUSt database. In proteobacteria, AMO has three subunits, AMO-A, AMO-B and AMO-C, with different sizes and structures. The AMO enzymes of nitrifying bacteria and in particular methane monooxygenase (pMMO) of methanotrophic bacteria are homologous and share many features. The structures of their operons are almost identical (Bothe et al., 2000). In heterotrophic nitrifier microorganisms, AMO enzymes were also found. However, this enzyme particularly for *Paracoccus pantotrophus* GB17 consists of only two subunits and has several features in common with the enzyme family which includes to AMO and pMMO (Bothe et al., 2000).

Nitrogen metabolism predicted by PYCRUSt involved different processes such as nitrification, nitrogen fixation, dissimilatory nitrate reduction and denitrification, which could take place in the system (Fig. 3). Good nitrifying activity took place since high nitrate concentration was generated. Nitrogen fixation can be considered of little relevance under the prevalent environmental conditions of excess ammonia in the system. Reduction of nitrate could take place in the aerobic SBR by means of dissimilatory nitrate reduction to ammonium (DNRA) and/or denitrification, although anoxic conditions are commonly required by these processes. It must be considered that most denitrifiers and some DNRA bacteria are aerobic, being able to switch to nitrate or nitrite reduction under anoxic conditions; many DNRA bacteria are anaerobes (Hardison et al., 2015). Competition by electron donors and electron acceptors (NO_3^--N and NO_2^--N) occurs between denitrifiers and DNRA bacteria. Thermodynamically, denitrification yields more free energy per electron and DNRA yields more free energy per molecule of nitrate than complete denitrification to N_2. Therefore, denitrification occurs commonly under electron donor-limiting conditions (i.e. low COD:NO_3^--N ratio), and DNRA occurs under NO_3-N--limiting conditions (i.e. high COD:NO_3^--N ratio) (Yoon et al., 2015; Chutivisut et al., 2018).

In the present study, denitrification was probably the most relevant process of nitrate reduction according to operational conditions and mass balances carried out. This hypothesis was supported by the following reasons: a) the reactor was operated at low COD:N ratio leading to relatively high levels of nitrate by nitrifying activity, b) external acetate, easily biodegradable carbon source, was mainly used for microbial growth and glycogen and PHA storage, c) nitrate reduction was mainly driven by intracellular carbon reserves. These conditions lead to non-limiting nitrate conditions (low COD:NO_3^--N ratio), which are favorable for denitrifying bacteria. Finally, the high oxygen concentrations favored the growth of aerobic denitrifiers, which can carry out the denitrification process in presence of oxygen.

A full nitrification process, involving ammonia oxidation followed by nitrite oxidation up to nitrate, was mainly carried out by heterotrophs although it is an energetically unfavorable process for these bacteria. It is known that the oxidation process of NH_4^+ coupled to denitrification of NO_2^-/NO_3^- by heterotrophic nitrifiers can contribute to the maintenance of cellular redox balance, by oxidation of excess NADH under hypoxia (Stein 2011). However, in the present study there was probably no low oxygen tension inside the granules because the high bulk oxygen levels (7.5 mg $O_2.L^{-1}$). Heterotrophic nitrifying activity more likely involved a detoxification mechanism of the environment against free ammonia. Denitrification from nitrate occurred.

Heterotrophic nitrification-aerobic denitrification (HNAD) was probably carried out by *Dyadobacter* sp. among other potential heterotrophic nitrifiers, and *Zoogloea* sp. and *Dechloromonas* sp. as aerobic denitrifiers. *Flavobacterium* sp. (Flavobacteriales) and *Diaphorobacter* sp. (Burkholderiales) found with high abundance in the system probably contributed to the HNAD process. *Flavobacterium* has been proposed as one of the microorganisms potentially responsible for HNAD process in granular SBR (Pishgar et al., 2019). Some strains of *Flavobacterium* and *Diaphorobacter* genera have demonstrated the ability to perform simultaneous nitrification and denitrification in pure cultures under aerobic conditions (Castignetti and Hollocher, 1984; Khardenavis et al., 2007). However, the active participation of these genera as HNAD bacteria in mixed cultures has yet to be proved. Autotrophic AOB and NOB could contribute to the nitrification process.

In the present study, high performance sequencing revealed the more abundant genera related to the process of biological nitrogen removal. Bioinformatic analysis and prediction of PYCRUSt provided potential key enzymes and metabolic routes of nitrogen transformation that could take place. HNAD was the main process responsible for the biological nitrogen removal. Analysis of main operating conditions (dissolved oxygen concentration and COD:NO_3^--N ratio) and NGS technology supported these results.

5. Conclusions

In an aerobic granular sequencing batch reactor (SBR), simultaneous nitrification and denitrification process (SND) occurred mainly in the starvation period with denitrification driven by PHA and glycogen according to the mass balance proposed.

Heterotrophic nitrifiers, NOB, AOB, HNAD bacteria and aerobic denitrifiers were detected by next generation sequencing (NGS) technology. Low COD:NO_3^--N ratio and high dissolved oxygen favored the growth of aerobic denitrifiers. Heterotrophic nitrification took place involving detoxification against ammonia. High abundance of HNAD bacteria, *Diaphorobacter* sp. and *Flavobacterium* sp., and *Zooglea* sp. aerobic denitrifier was detected. *Dyadobacter* sp. was a relevant microorganism of the microbial community with probable nitrifying activity. Autotrophic nitrifiers showed lower relative abundance.

HNAD was the main process responsible for the biological nitrogen removal according to NGS and operating conditions.

Declaration of competing interest

The authors declare that they have no known competing financial interests or personal relationships that could have appeared to influence the work reported in this paper.

Acknowledgments

The authors gratefully acknowledge the financial support given by the Consejo Nacional de Investigaciones Científicas y Técnicas (CONICET), Universidad Nacional de La Plata, and Agencia Nacional de Promoción Científica y Tecnológica, ARGENTINA.

Appendix A. Supplementary data

Supplementary data to this article can be found online at https://doi.org/10.1016/j.ibiod.2021.105210.

References

Barman, P., Kati, A., Mandal, A.K., Bandyopadhyay, P., 2017. Mohapatra P.K.D. Biopotentiality of *Bacillus cereus* PB45 for nitrogenous waste detoxification in ex situ model. Aquacult. Int. 25, 1167–1183. https://doi.org/10.1007/s10499-016-0105.

Baskaran, V., Patil, P.K., Antony, M.L., 2020. Microbial community profiling of ammonia and nitrite oxidizing bacterial enrichments from brackishwater ecosystems for mitigating nitrogen species. Sci. Rep. 10, 5201. https://doi.org/10.1038/s41598-020-62183-9.

Bothe, H., Jost, G., Schloter, M., Ward, B.B., Witzel, K.P., 2000. Molecular analysis of ammonia oxidation and denitrification in natural environments. FEMS (Fed. Eur. Microbiol. Soc.) Microbiol. Rev. 24, 673–690.

Bucci, P., Coppotelli, B., Morelli, I., Zaritzky, N., Caravelli, A., 2020. Simultaneous heterotrophic nitrification and aerobic denitrification of wastewater in granular reactor: microbial composition by next generation sequencing analysis. J. Water Process Eng. 36, 101254. https://doi.org/10.1016/j.jwpe.2020.101254.

Caporaso, J.G., Kuczynski, J., Stombaugh, J., 2010. QIIME allows analysis of high-throughput community sequencing data. Nat. Methods 7 (5), 335–336. https://doi.org/10.1038/nmeth.f.303.

Castignetti, D., Hollocher, T.C., 1984. Heterotrophic nitrification among denitrifiers. Appl. Environ. Microbiol. 47, 620–623.

Chai, H., Xiang, Y., Chen, R., Shao, Z., Gu, L., Li, L., He, Q., 2019. Enhanced simultaneous nitrification and denitrification in treating low carbon-to-nitrogen ratio wastewater: treatment performance and nitrogen removal pathway. Bioresour. Technol. 280, 51–58.

Chutivisut, P., Isobe, K., Powtongsook, S., Pungrasmi, W., Kurisu, F., 2018. Distinct microbial community performing dissimilatory nitrate reduction to ammonium (DNRA) in a high C/NO_3^- reactor. Microb. Environ. 33 (3), 264–271. https://doi.org/10.1264/jsme2.ME17193.

Comeau, A.M., Douglas, G.M., Langille, M.G.I., 2017. Microbiome helper: a custom and streamlined workflow for microbiome research. mSystems 2. https://doi.org/10.1128/mSystems e00127–e00116.

Deng, M., Dai, Z., Senbati, Y., Li, L., Song, K., He, X., 2020. Aerobic denitrification microbial community and function in zero-discharge recirculating aquaculture system using a single biofloc-based suspended growth reactor: influence of the carbon-to-nitrogen ratio. Front. Microbiol. 11, 1760. https://doi.org/10.3389/fmicb.2020.01760.

De Voogd, N.J., Cleary, D.F.R., Polónia, A.R.M., Gomes, N.C.M., 2015. Bacterial community composition and predicted functional ecology of sponges, sediment and seawater from the thousand islands reef complex, West Java, Indonesia. FEMS (Fed. Eur. Microbiol. Soc.) Microbiol. Ecol. 91, 1–12.

Edgar, R.C., Haas, B.J., Clemente, J.C., Quince, C., Knight, R., 2011. UCHIME improves sensitivity and speed of chimera detection. Bioinformatics 27, 2194–2200. https://doi.org/10.1093/bioinformatics/btr381.

Gernaey, K., Petersen, B., Nopens, I., Comeau, Y., Vanrolleghem, P.A., 2002. Modelling aerobic carbon source degradation processes using titrimetric data and combined respirometric-titrimetric data: I. Experimental data and model structure. Biotechnol. Bioeng. 79, 741–753.

Guisasola, A., Vargas, M., Marcelino, M., Lafuente, J., Casas, C., Baeza, J.A., 2007. On-line monitoring of the enhanced biological phosphorus removal process using respirometry and titrimetry. Biochem. Eng. J. 35, 371–379.

Han, H., Song, B., Song, M.J., Yoon, S., 2019. Enhanced nitrous oxide production in denitrifying *Dechloromonas aromatica* strain RCB under salt or alkaline stress conditions. Front. Microbiol. 10, 1203.

Hardison, A.K., Algar, C.K., Giblin, A.E., Rich, J.J., 2015. Influence of organic carbon and nitrate loading on partitioning between dissimilatory nitrate reduction to ammonium (DNRA) and N_2 production. Geochem. Cosmochim. Acta 164, 146–160.

Harun, H., Anuar, A.N., Halim, M.H.A., Othman, I., Rosman, N.H., Hamid, N.H.A., Ujang, Z., van Loosdrecht, M., 2020. Granulation and biodegradation by microbial species in granular sequencing batch reactor for soy sauce wastewater treatment. In: Zakaria, Z., Boopathy, R., Dib, J. (Eds.), Valorisation of Agro-Industrial Residues – Volume I: Biological Approaches. Applied Environmental Science and Engineering for a Sustainable Future. Springer, Cham. https://doi.org/10.1007/978-3-030-39137-9_14.

Huang, X., Li, W., Zhang, D., Qin, W., 2013. Ammonium removal by a novel oligotrophic *Acinetobacter* sp. Y16 capable of heterotrophic nitrification–aerobic denitrification at low temperature. Bioresour. Technol. 146, 44–50.

Huang, T., Guo, L., Zhang, H., Su, J., Wen, G., Zhang, K., 2015. Nitrogen-removal efficiency of a novel aerobic denitrifying bacterium, Pseudomonas stutzeri strain ZF31, isolated from a drinking-water reservoir. Bioresour. Technol. 196, 209–216.

Jin, P., Chen, Y., Yao, R., Zheng, Z., Du, Q., 2019. New insight into the nitrogen metabolism of simultaneous heterotrophic nitrification-aerobic denitrification bacterium in mRNA expression. J. Hazard Mater. 371, 295–303.

Kanehisa, M., Goto, S., Sato, Y., Furumichi, M., Tanabe, M., 2012. KEGG for integration and interpretation of large-scale molecular data sets. Nucleic Acids Res. 40, D109–D114.

Khanichaidecha, A., Nakaruk, K., Ratananikom, R., Kazama, Eamrat F., 2019. Heterotrophic nitrification and aerobic denitrification using pure-culture bacteria for wastewater treatment. J. Water Reuse Desalination 9 (1), 10–17.

Khardenavis, A.A., Kapley, A., Purohit, H.J., 2007. Simultaneous nitrification and denitrification by diverse Diaphorobacter sp. Appl. Microbiol. Biotechnol. 77, 403–409.

Kim, D., Hofstaedter, C.E., Zhao, C., Mattei, L., Tanes, C., Clarke, E., Conrad, M., 2017. Optimizing methods and dodging pitfalls in microbiome research. Microbiome 5, 52.

Kopylova, E., Noé, L., Touzet, H., 2012. SortMeRNA: fast and accurate filtering of ribosomal RNAs in metatranscriptomic data. Bioinformatics 28, 3211–3217.

Lang, X., Li, Q., Xu, Y., Ji, M., Yan, G., Guo, S., 2019. Aerobic denitrifiers with petroleum metabolizing ability isolated from caprolactam sewage treatment pool. Bioresour. Technol. 290, 121719.

Langenheder, S., Bulling, M.T., Solan, M., Prosser, J.I., 2010. Bacterial biodiversity-ecosystem functioning relations are modified by environmental complexity. PloS One 5.

Langille, M.G.I., Zaneveld, J., Caporaso, J.G., McDonald, D., Knights, D., Reyes, J.A., Clemente, J.C., Burkepile, D.E., Vega Thurber, R.L., Knight, R., Beiko, R.G., Huttenhower, C., 2013. Predictive functional profiling of microbial communities using 16S rRNA marker gene sequences. Nat. Biotechnol. 31, 814–821. https://doi.org/10.1038/nbt.2676.

Lei, Y., Wang, Y., Liu, H., Xi, C., Song, L., 2016. A novel heterotrophic nitrifying and aerobic denitrifying bacterium, *Zobellella taiwanensis* DN-7, can remove high-strength ammonium. Appl. Microbiol. Biotechnol. 100, 4219–4229. https://doi.org/10.1007/s00253-016-7290-5.

Li, H., Zhang, Y., Li, D., Xu, H., Chen, G., Zhnag, C., 2009. Comparisons of different hypervariable regions of rrs genes for fingerprinting of microbial communities in paddy soils. Soil Biol. Biochem. 41, 954–958.

Li, D., Liang, X., Jin, Y., Wu, C., Zhou, R., 2019a. Isolation and nitrogen removal characteristics of an aerobic heterotrophic nitrifying-denitrifying bacterium, *Klebsiella* sp. TN-10. Appl. Biochem. Biotechnol. 188, 540–554. https://doi.org/10.1007/s12010-018-02932-9.

Li, D., Zhang, S., Li, S., Zeng, H., Zhang, J., 2019b. The nitrogen removal of autotrophic and heterotrophic bacteria in aerobic granular reactors with different feast/famine ratio. Bioresour. Technol. 272, 370–378.

Liu, X., Shu, Z., Sun, D., Dang, Y., Holmes, D.E., 2018. Heterotrophic nitrifiers dominate reactors treating incineration leachate with high free ammonia concentrations. *ACS* Sustain. Chem. Eng. 6, 15040–15049.

Massone, A., Gernaey, K., Rozzi, A., Verstraete, W., 1998. Measurement of ammonium concentration and nitrification rate by a new titrimetric biosensor. Water Environ. Res. 70, 343–350.

Mercier, C., Boyer, F., Bonin, A., Coissac, E., 2013. SUMATRA and SUMACLUST: fast and exact comparison and clustering of sequences. Available. https://git.metabarcoding.org/obitools/ sumaclust.

Mori, J.F., Chen, L.X., Jessen, G.L., Rudderham, S.B., McBeth, J.M., Lindsay, M.B.J., Slater, G.F., Banfield, J.F., Warren, L.A., 2019. Putative mixotrophic nitrifying-denitrifying gammaproteobacteria implicated in nitrogen cycling within the ammonia/oxygen transition zone of an oil sands pit lake. Front. Microbiol. 10 https://doi.org/10.3389/fmicb.2019.02435. Article 2435.

Neissi, A., Rafiee, G., Farahmand, H., Rahimi, S., Mijakovic, I., 2020. Cold-resistant heterotrophic ammonium and nitrite-removing bacteria improve aquaculture conditions of rainbow trout (*Oncorhynchus mykiss*). Microb. Ecol. 80, 266–277.

Pacheco-Sánchez, D., Rama-Garda, R., Marín, P., Martirani-Von Abercron, S.-M., Marqués, S., 2019. Occurrence and diversity of the oxidative hydroxyhydroquinone pathway for the anaerobic degradation of aromatic compounds in nitrate-reducing bacteria. Environ. Microbiol. Rep. 11, 525–537.

Padhi, S., Das, D., Panja, S., Tayung, K., 2017. Molecular characterization and antimicrobial activity of an endolichenic fungus, Aspergillus sp. isolated from Parmelia caperata of Similipal Biosphere Reserve, India. Interdiscipl. Sci. 9, 237–24.

Pal, R.R., Khardenavis, A.A., Purohit, H.J., 2015. Identification and monitoring of nitrification and denitrification genes in *Klebsiella pneumoniae* EGD-HP19-C for its ability to perform heterotrophic nitrification and aerobic denitrification. Funct. Integr. Genom. 15 (1), 63–76. https://doi.org/10.1007/s10142-014-0406-z.

Parks, D.H., Tyson, G.W., Hugenholtz, P., Beiko, R.G., 2014. STAMP: statistical analysis of taxonomic and functional profiles. Bioinformatics 30, 3123–3124. https://doi.org/10.1093/bioinformatics/btu494.

Petersen, B., Gernaey, k., Vanrolleghem, P.A., 2002. Anoxic activated sludge monitoring with combined nitrate and titrimetric measurements. Water Sci. Technol. 45, 181–190.

Philips, S., Laanbroek, H.J., Verstraete, W., 2002. Origin, causes and effects of increased nitrite concentrations in aquatic environments. Rev. Environ. Sci. Biotechnol. 1, 115–141.

Pishgar, R., Dominic, J.A., Sheng, Z., Tay, J.H., 2019. Denitrification performance and microbial versatility in response to different selection pressures. Bioresour. Technol. 281, 72–83.

Pratt, S., Yuan, Z., Keller, J., 2004. Modeling aerobic carbon oxidation and storage by integrating respirometric, titrimetric, and off-gas CO_2 measurements. Biotechnol. Bioeng. 88, 135–147.

Rognes, T., Flouri, T., Nichols, B., Quince, C., Mahé, F., 2016. VSEARCH: a versatile open source tool for metagenomics. PeerJ 4, e2584.

Saijai, S., Ando, A., Inukai, R., Shinohara, M., Ogawa, J., 2016. Analysis of microbial community and nitrogen transition with enriched nitrifyng soil microbes for organic hydroponics. Biosci. Biotechnol. Biochem. 80, 2247–2254.

Silva, L.C.F., Lima, H.S., de Oliveira Mendes, T.A., Sartoratto, A., de Paula Sousa, M., de Souza, R.S., Oliveira de Paula, S., de Oliveira, V.M., Canêdo da Silva, C., 2019. Heterotrophic nitrifying/aerobic denitrifying bacteria: ammonium removal under different physical-chemical conditions and molecular characterization. J. Environ. Manag. 248, 109294.

Stein, L.Y., 2011. Heterotrophic nitrification and nitrifier denitrification. Nitrification 95–114.

Third, K.A., Burnett, N., Cord-Ruwisch, R., 2003a. Simultaneous nitrification and denitrification using stored substrate (PHB) as the electron donor in an SBR. Biotechnol. Bioeng. 83, 706–720.

Third, K.A., Newland, M., Cord-Ruwisch, R., 2003b. The effect of dissolved oxygen on PHB accumulation in activated sludge cultures. Biotechnol. Bioeng. 82, 238–250, 2003.

Vadivelu, V.M., Keller, J., Yuan, Z., 2007. Free ammonia and free nitrous acid inhibition on the anabolic and catabolic processes of *Nitrosomonas* and *Nitrobacter*. Water Sci. Technol. 56, 89–97.

Venkateswar Reddy, M., Nikhil, G.N., Venkata Mohan, S., Swamy, Y.V., Sarma, P.N., 2012. *Pseudomonas otitidis* as a potential biocatalyst for polyhydroxyalkanoates (PHA) synthesis using synthetic wastewater and acidogenic effluents. Bioresour. Technol. 123, 471–479.

Wang, T., Li, J., Zhang, L.H., Yu, Y., Zhu, Y.M., 2017. Simultaneous heterotrophic nitrification and aerobic denitrification at high concentrations of NaCl and ammonia nitrogen by *Halomonas* bacteria. Water Sci. Technol. 76, 386–395.

Yang, J., Liu, X., Wang, D., Xu, Q., Yang, Q., Zeng, G., Li, X., Liu, Y., Gong, J., Ye, J., 2019. Mechanisms of peroxymonosulfate pretreatment enhancing production of short-chain fatty acids from waste activated sludge. Water Res. 148, 239–249.

Yoon, S., Cruz-García, C., Sanford, R., Ritalahti, K.M., Frank, E., Löffler, F.E., 2015. Denitrification versus respiratory ammonification: environmental controls of two competing dissimilatory NO_3^-/NO_2^- reduction pathways in *Shewanella loihica* strain PV-4. ISME J. 9, 1093–1104.

Zhang, J., Kobert, K., Flouri, T., 2014. Stamatakis A. PEAR: a fast and accurate Illumina paired-end reAd mergeR. Bioinformatics 30, 614–620.

Zhang, S., Sun, X., Fan, Y., Qiu, T., Gao, M., Wang, X., 2017. Heterotrophic nitrification and aerobic denitrification by *Diaphorobacter polyhydroxybutyrativorans* SL-205 using poly(3-hydroxybutyrate- co -3-hydroxyvalerate) as the sole carbon source. Bioresour. Technol. 241, 500–507. https://doi.org/10.1016/j.biortech.2017.05.185.

Zhao, B., An, Q., He, Y.L., Guo, J.S., 2012. N_2O and N_2 production during heterotrophic nitrification by Alcaligenes faecalis strain NR. Bioresour. Technol. 116, 379–385.

Zhao, Y., Huang, J., Zhao, H., Yang, H., 2013. Microbial community and N removal of aerobic granular sludge at high COD and N loading rates. Bioresour. Technol. 143, 439–446.

Zheng, X., Tong, J., Li, H., Chen, Y., 2009. The investigation of effect of organic carbon sources addition in anaerobic-aerobic (low dissolved oxygen) sequencing batch reactor for nutrients removal from wastewaters. Bioresour. Technol. 100, 2515–2520.